POWER SEMICONDUCTORS DEVICES FOR INDUSTRIAL PWM INVERTERS: STATE OF ART

Gianluca Sena*, Roberto Marani** and Anna Gina Perri*

* Electronic Devices Laboratory, Department of Electrical and Information Engineering,
Polytechnic University of Bari, via E. Orabona 4, Bari – Italy
** Consiglio Nazionale delle Ricerche, Istituto di Studi sui Sistemi Intelligenti per
l'Automazione (ISSIA), Bari, Italy

ABSTRACT

In this paper the state of art of semiconductors devices for Industrial Pulse-Width Modulation (PWM) Inverters is presented. The last generations of Insulated Gate Bipolar Transistors (IGBTs), Silicon Carbide (SiC) MOSFETs and Gallium Nitride (GaN) Transistors are introduced and analysed. At last a comparison between Si-based IGBT and SiC MOSFET, obtained by SPICE simulations, is presented in order to identify the device which makes the PWM inverter more efficient.

KEYWORDS: Power semiconductor devices, PWM Inverter, SiC MOSFETs, IGBTs, SPICE simulation.

I. INTRODUCTION

New global energy needs have led to changes in the industrial environments. Pollution restrictions, costs reductions and the rising demand for energy have been translated into efficiency requirements of the energy conversion systems and of the electrical drives. Both these systems are based on Pulse-Width Modulation (PWM) Inverter [1].

PWM is the process of modifying the width of the pulses in a pulse train in direct proportion to a control signal. Depending on how the duty cycle is modified, it determines the specific type of the modulation. In Sinusoidal PWM (SPWM), by using a sine wave of the desired frequency as control voltage for PWM circuit, it is possible to produce a high-power waveform whose average voltage varies sinusoidally [2]. Low pass filtering a SPWM waveform produces an output voltage whose amplitude is proportional to the duty cycle of the pulse train. To produce the SPWM signal we compare a sine wave with a reference triangular wave as shown in Fig.1.
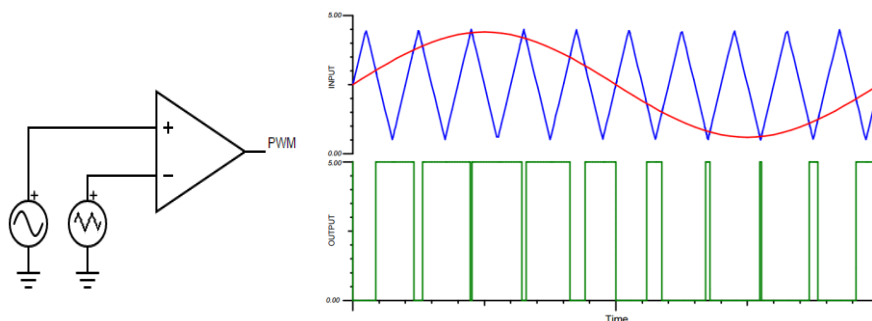

Figure 1. The output of a comparator (green) with a triangle wave applied to its negative input (blue) and a sine wave applied to its positive input (red) (*from [3]*).

When the value of the triangle wave is greater than the value of the input signal, the output of the comparator is low; when the value of the input signal is greater than that of the triangle wave, the output of the comparator is high. This simple method produces an output square wave with a duty cycle that varies depending on an input voltage. [3]

PWM Inverter converts a DC power into an AC power, generically this AC power is a three-phases AC power. The input DC voltage is obtained from the electrical grid through (active or passive) rectification, or from a DC supply e.g. storage battery or photovoltaic panel. The conversion of DC power to three-phase AC power is exclusively performed in the switched mode with Pulse-Width Modulation. In Fig. 2 three-phase two-levels PWM inverter is shown.
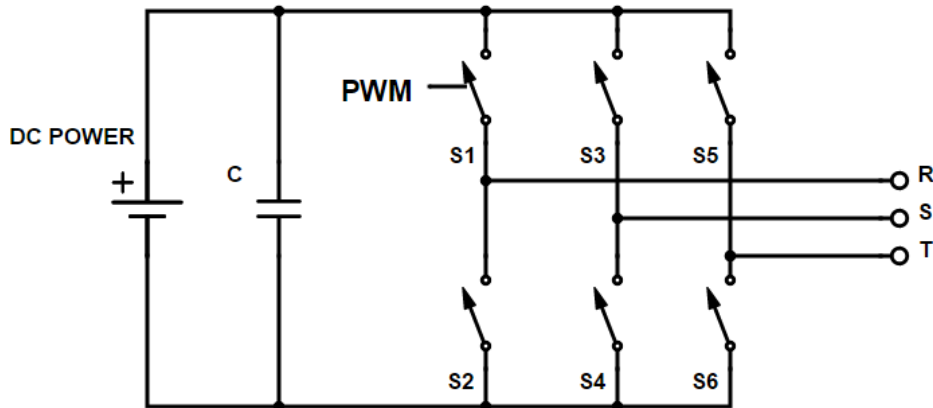

Figure 2. Principle circuit diagram of three-phase two-levels PWM inverter.

The six switches are six power semiconductor devices driven by low voltage PWM signals that make temporary connections at high repetition rates between the two DC terminals and the three phases of the AC device, usually a motor, connected to the output of the inverter. The desired value of the AC currents is achieved by varying the duty cycles of the six PWM signals [4].

To improve the energy requirements, we need to make the PWM inverter more efficient. There are many types of techniques to achieve that. Soft switching techniques, different topologies of inverters and many kinds of control algorithms are constantly subject matter of research. Last but not least, also the power semiconductors switches are constantly evolving because represent the primary causes of energy dissipation: improving these devices means reducing thermal heating or the reactive losses [5-6].

The presentation of the paper is organized as follows. In Section II we present the state of art of semiconductors devices for Industrial PWM Inverters, while in Section III the last generations of Insulated Gate Bipolar Transistors (IGBTs), Silicon Carbide (SiC) MOSFETs and Gallium Nitride (GaN) Transistors are introduced and analysed. In Section IV, a comparison between Si-based IGBT and SiC MOSFET, obtained by SPICE simulations, is presented in order to identify the device which makes the PWM inverter more efficient. At last, the conclusions are described in Section V.

II.   4H–SiC STEP TRENCH GATE POWER MOSFET

2 a) Power MOSFET and Trench Gate Structure

In a traditional n-channel MOSFET, lateral MOSFET, the saturation drain current, I_{Dsat}, is given by the following equation [7-8]:

$$I_{Dsat} = \mu_n C_{oss} \frac{W}{2L} (V_G - V_T)^2$$

where μ_n is the electron mobility, C_{ox} is the oxide capacitance, W and L are the width and the channel length respectively, V_{GS} is the gate-source voltage and V_T is the threshold voltage.

To increase the MOSFET currents, we need to made W large and L small. On the other hand, reducing L, we have a reduction of the breakdown voltage. When the body-to-drain junction is reverse polarized, the depletion region spreads into short channel, resulting in breakdown at relatively low voltage. This effect limits the lateral MOSFET in high voltage applications [9].

Planar MOSFET (Fig. 3a, [10]), also known as DMOSFET (double diffused), has been developed to obtain short channel. The channel is formed on the surface by the double-diffusion process and the relative diffusion depth of the P body and N+ source regions control the channel length [11]. The current flows vertically, from drain to source, crossing N drift region. Due to the two adjacent P body wells, the current was affected by the JFET-effect when flows in N- drift region [10].
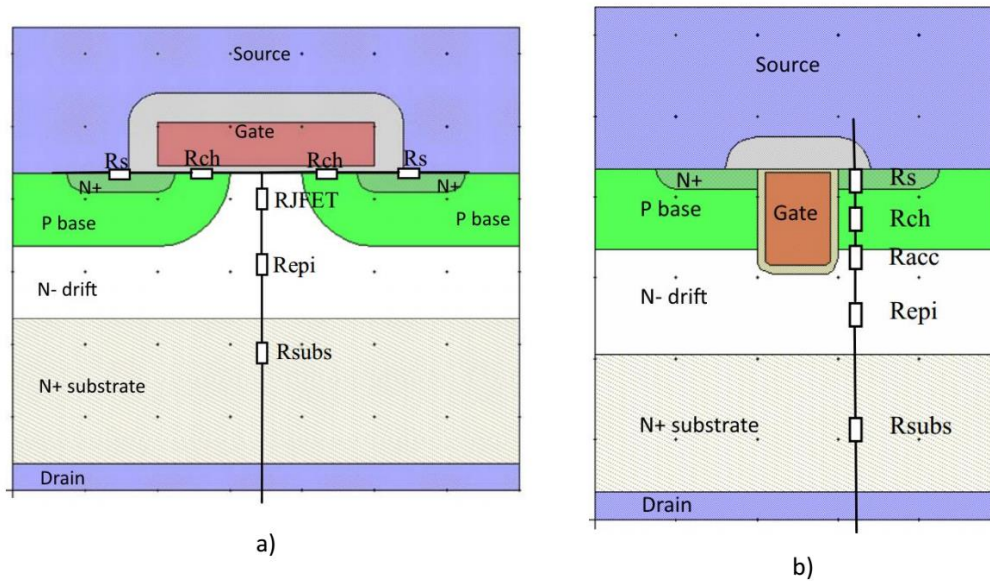
Figure 3. DMOSFET (a) and Trench Gate MOSFET (b) with R_{DS} components (*from [10]*).

In the trench-gate structure (Fig. 3b) the gate is etched vertically along the device and the channel is formed on the vertical sidewalls of the trench and the JFET resistance is reduced drastically [10-11].

2 b) Silicon Carbide and the newest SiC Power MOSFET

The Silicon Carbide (SiC), as Silicon (Si), is a semiconductor material but, compared with the latter, offers: a lower intrinsic carrier concentration (9–18 orders of magnitude), a higher electric breakdown field (4–8 times) that allows a ten times reduction in drift layer thickness, a higher thermal conductivity that allows high temperature operation up to 350°C, a larger saturated electron drift velocity that allows the increasing of the switching frequency. Due to difficulty with material processing and presence of crystal defects, silicon carbide has been adopted for power devices only in the last years after the improvement of the fabrication processes. Only the 6H– and 4H–SiC poly-types are available commercially but 4H–SiC is preferred in power devices fabrication because of its high carrier mobility and its low dopant ionization energy [12].

The new generation of SiC Power MOSFET presented in [13] is developed with 4H-SiC because this material has 10X higher breakdown strength when compared to silicon, leading to realize a 10kV devices. With SiC technology R_{DS}, total current per die and switching losses per chip are improved. Furthermore, trench gate technology allows better performance in matter of conduction losses.

III. 7ᵀᴴ GENERATION TRENCH GATE PUNCH THROUGH IGBT

3 a) IGBT and Punch-Trough Technology

An IGBT combines the advantages of MOSFETs and BJTs. MOSFETs have high switching frequency and are voltage controlled but their internal resistance growing with applied voltage. BJTs instead, have a low voltage drop but requires a current as input control signal. IGBT is a voltage-controlled device, it has a low voltage drop and it is fast for switching operations. If we analyse a traditional IGBT we can see that its structures are similar to that of vertical MOSFET (DMOS) where N+ interface is replaced by P+ substrate (Fig. 4) [14].
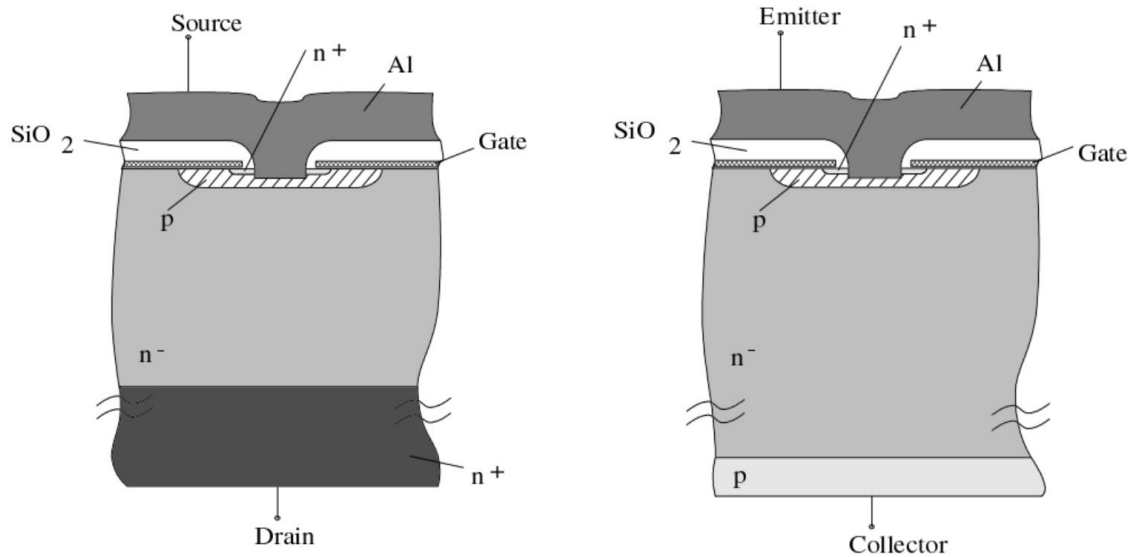
Figure 4. Power MOSFET(left) IGBT (right) (*from [15]*).

This configuration is also called Not Punch Trough (NPT), shown in Fig. 5.
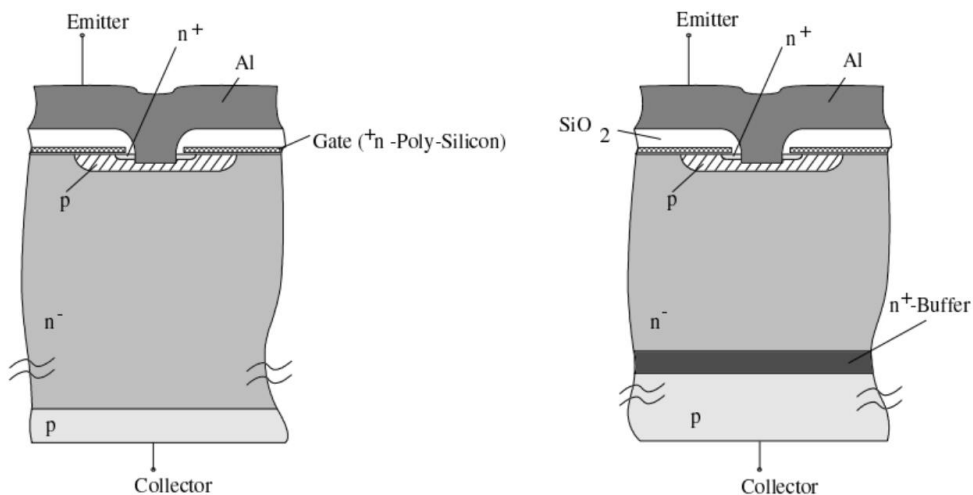
Figure 5. NPT (left) and PT (right) IGBT (*from [13]*).

A NPT IGBT presents two main drawbacks for switching applications: it has equal forward and reverse breakdown voltages and presents a long tail current (due to the storage charge in N-drift region). To solve these problems, Punch Trough (PT) technology has been developed. PT structure is obtained adding a N+ substrate in NPT IGBT between P+ substrate and N– drift region. The new N+ region is a buffer layer that makes the P+N– diode like a PIN type diode: the carrier lifetime is reduced (consequently the tail current is reduced) and it provides a reverse breakdown voltage greater than the forward breakdown voltage despite the increase of voltage drop during the ON-state [14] [15] [16].

3 b) The Newest generation of IGBT

The 7th generation of IGBT, as described in [17], is shown in Fig. 6 and represents the newest generation of Trench Gate Punch Through IGBT.
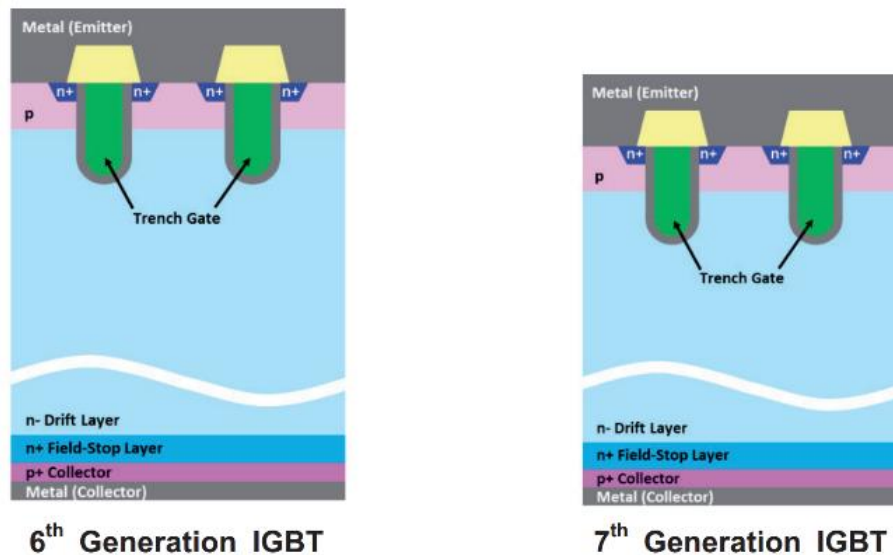
Figure 6. Cross-sections of the 6th generation IGBT and the 7th generation IGBT (*from [17]*).

Compared to previous generation, the electrical characteristics have been improved, the die size has been reduced and higher efficiency was achieved. This technology leads to a new generation of highly compact and efficient power conversion systems.
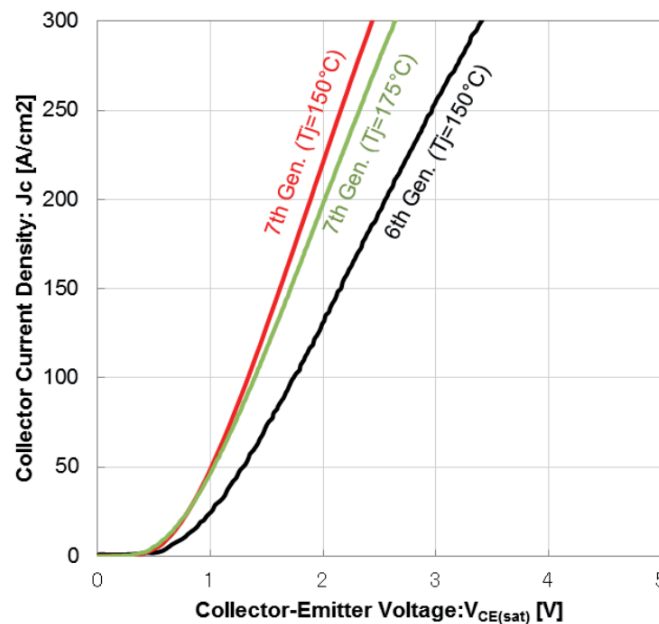The drift layer thickness is reduced compared to the 6th generation achieving a lower on-state voltage (Fig. 7) drop and a reduction of the Miller capacitor.

Figure 7 – The output characteristics of 7th and 6th generations IGBT (*from [17]*).

Additionally, the trade-off relationship between on-state voltage drop and turn-off losses is improved (Fig. 8) by optimization of the surface structure.
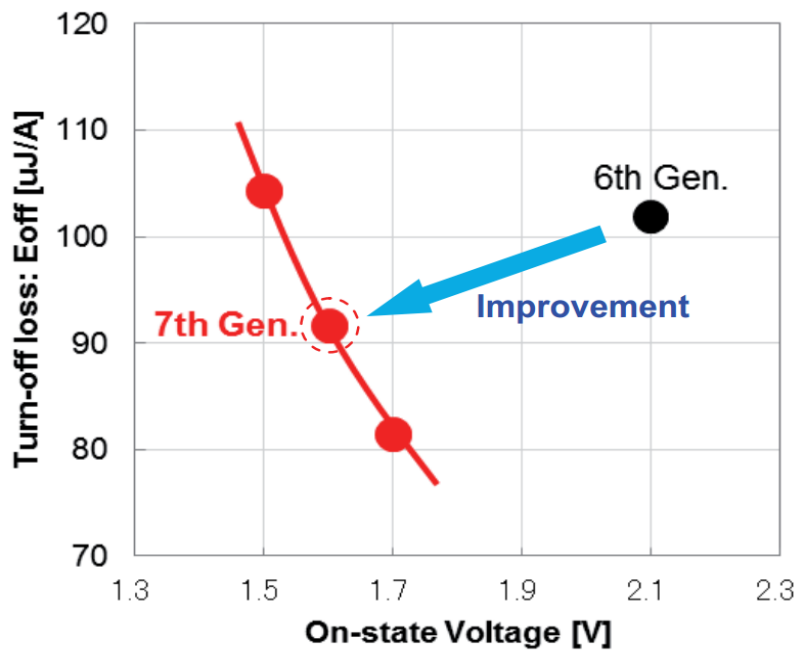Furthermore, the Injection Enhanced (IE) effects is increased and on-state voltage drop is decreased.

Figure 8. The trade-off relationship between turnoff losses and on-state voltage drop (*from [17]*).

The turn-off switching losses is reduced and waveforms are shown in Fig. 9.
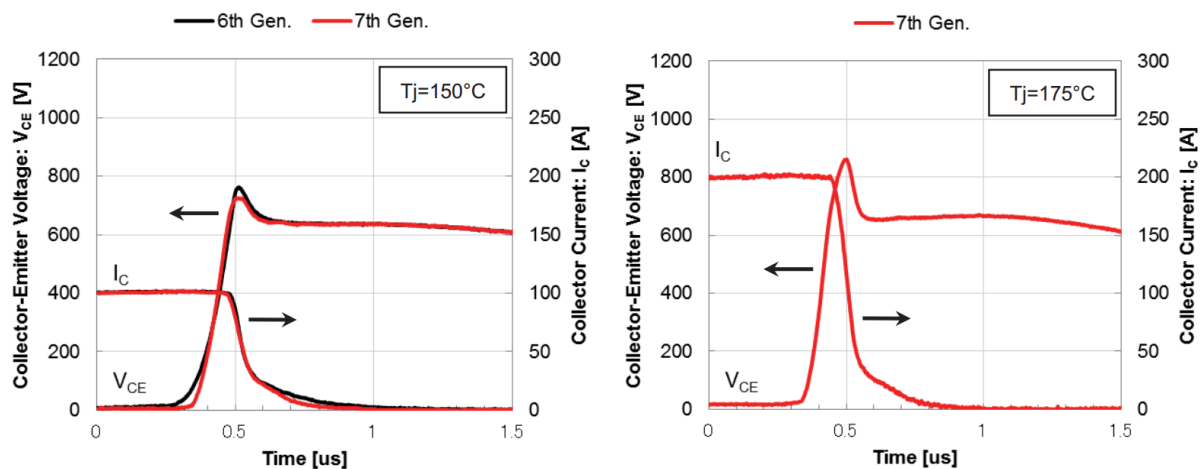These solutions improve also the thermal stability.

Figure 9. Turn-off switching waveforms of 7th and 6th generations IGBT (*from [17]*).

The Field Stop layer have been optimized, realizing the suppression of voltage oscillations and improving the breakdown voltage capability. The leakage current of the 7th generation IGBT is less than 28% compared to the 6th generation IGBT (VCE=1200V and Tj=150 °C). The reduction of the drift layer has led to the reducing of the forward voltage of the 7th generation diode as shown in Fig. 10.
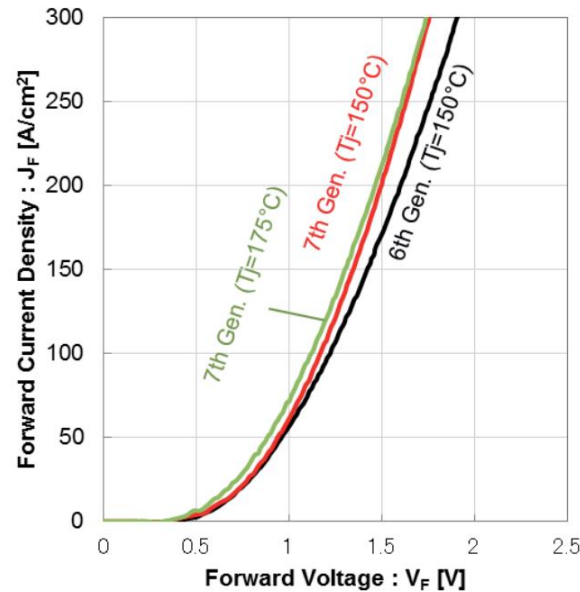
Figure 10. Output characteristics of 7th and 6th generations Diode (*from [17]*).

By optimization of the local lifetime control, the 7th generation diode realized a softer switching waveform, contributing to reduction of the reverse recovery losses (Fig. 11) [17].
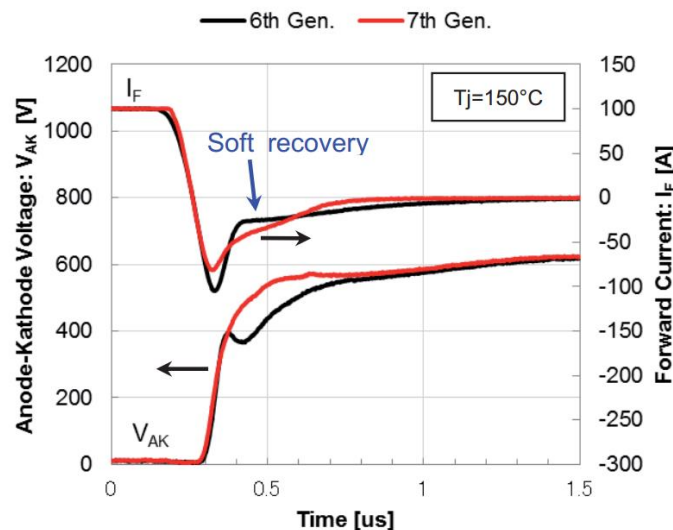

Figure 11. Reverse recovery switching waveforms of 7th gen. diode and 6th gen. diode. Switching conditions: Tj=150°C, VCC=600V, IC=100A (1x I_{NOM}), VGE=+15V/-15V (*from [17]*).

IV.   SiC-Based MOSFET Vs Si-Based IGBT

In this section we present a comparative evaluation, through static and dynamic results, obtained for SiC-MOSFET (ST STGW15H120DF2 [18]) and Si-IGBT (ST SCT20N120 [19]) with the same 1200 V voltage rating and similar current rating, 15 A of IGBT and 20 A of MOSFET. Both power devices have an intrinsic recovery anti-parallel diode. In order to characterize the switching performance of the devices, a real test-bed is simulated using values estimated in [20].
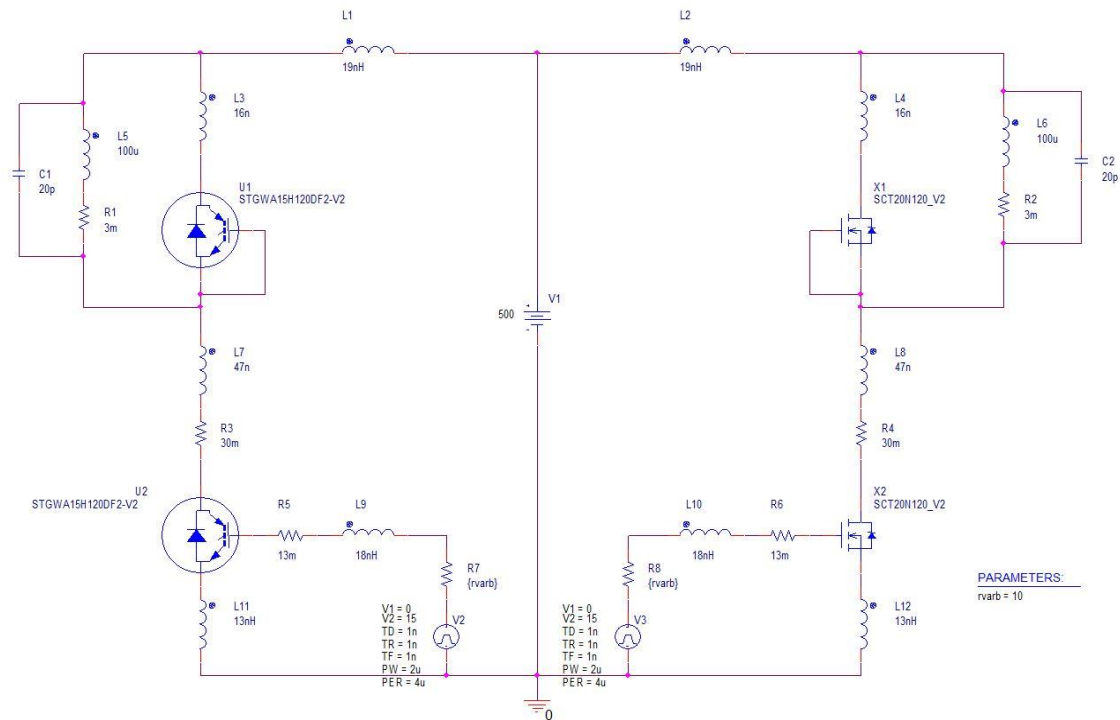The equivalent test circuit is shown in Fig. 12.

Figure 12. Test circuit.

A 100 uH inductor is used as test load with 20pF EPC and 3mΩ ESR. Testes exposed in [21] were used as guidelines for our simulations.

4 a) Static Characterization

Fig. 13 shows the transfer characteristics at various V_{CE}/V_{DS} using 10 Ω gate resistance at the junction temperature of 125 °C. Solid lines with square symbols show IGBT characteristics (I_C vs V_{GE}) and dashed lines with "x" symbols show MOSFET characteristics (I_D vs V_{GS}).

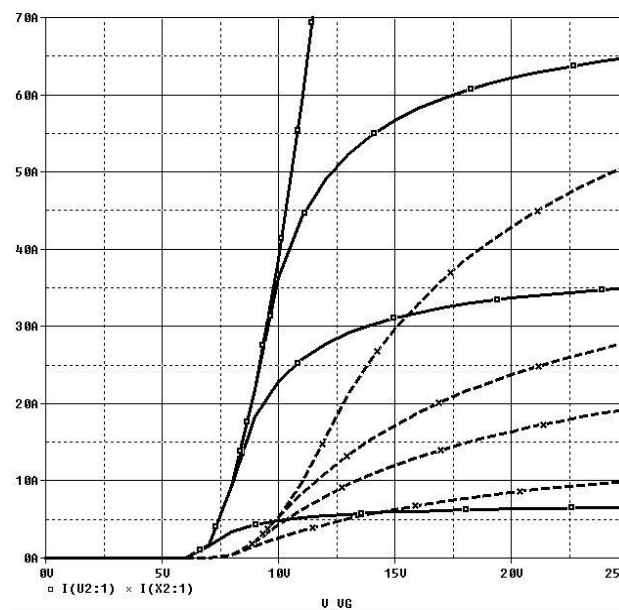**Figure 13.** Transfer characteristics.

Similarly Fig. 14 shows the output characteristics at various gate bias using 10 Ω gate resistance at the junction temperature of 125 °C. Solid lines with square symbols show IGBT characteristics (I_C vs V_{CE}) and dashed lines with "x" symbols show MOSFET characteristics (I_D vs V_{DS}).
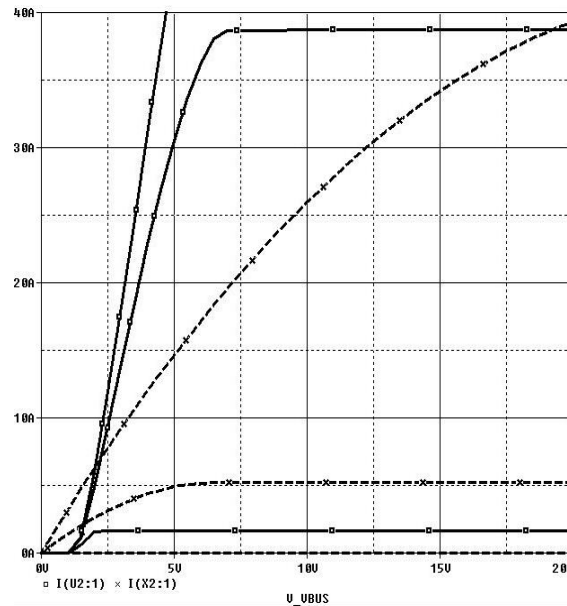

Figure 14. Output characteristics.

4 b) Dynamic Characterization
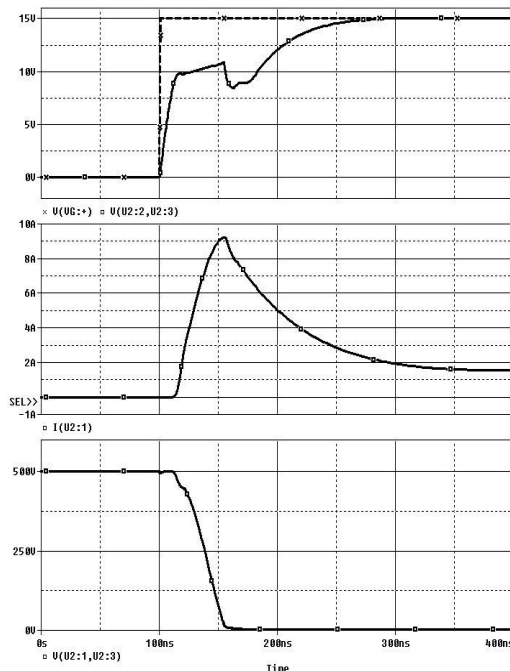The dynamic characteristics of the simulated IGBT are shown in Figures 15 and 16.

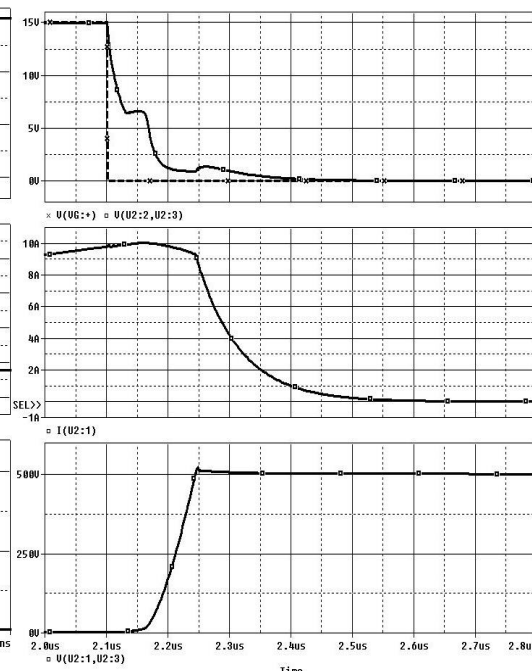**Figure 15.** IGBT turn-on.   **Figure 16.** IGBT turn-off.

In particular in Fig. 15 we have highlighted the turn-on behaviour, while in Fig. 16 the turn-off behaviour is highlighted. Top graphs present the driving voltage as dashed line and V_{GE} as solid line. In middle graphs collector current is shown and bottom graphs present the V_{CE}. The driving pulse had 2 µs pulse and a 4 µs period at the junction temperature of 125 °C.

Similarly the dynamic characteristics of the simulated MOSFET are shown in Figures 17 and 18.
In particular Fig. 17 shows the turn-on behaviour, while in Fig. 18 the turn-off behaviour is highlighted. Top graphs presents the driving voltage as dashed line and V_{GS} as solid line. In middle graphs drain current is shown and bottom graphs present the V_{DS}. The driving pulse had 2 µs pulse and a 4 µs period at the junction temperature of 125°C.
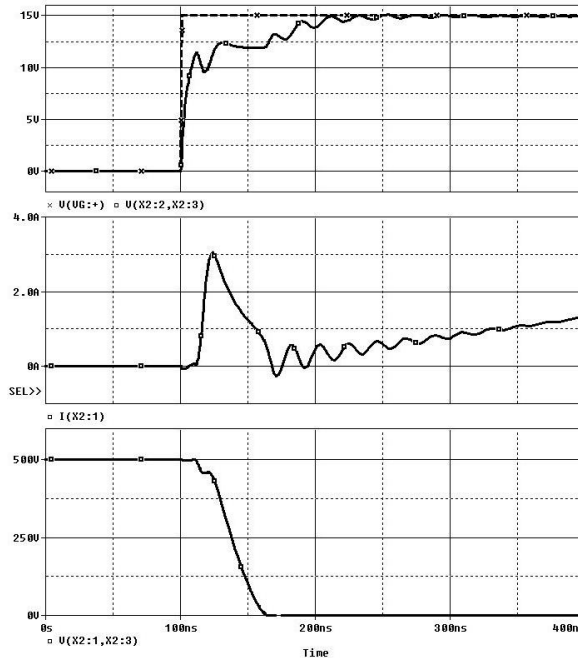

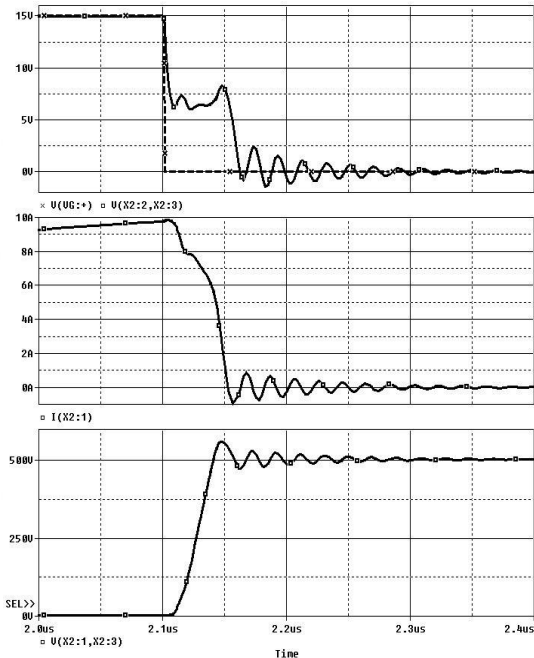**Figure 17.** MOSFET turn-on.   **Figure 18.** MOSFET turn-off.

Fig. 19 compares IGBT (a) and MOSFET (b) turn-on dynamics at various gate resistance. On the top the current is shown, on the bottom the V_{GE}/V_{GS}. Solid lines are referred to RG = 5 Ω, dashed lines are referred to RG = 10 Ω and dotted lines are referred to RG = 20 Ω. The higher the gate resistance, the smoother the characteristics but turn-on time increases.

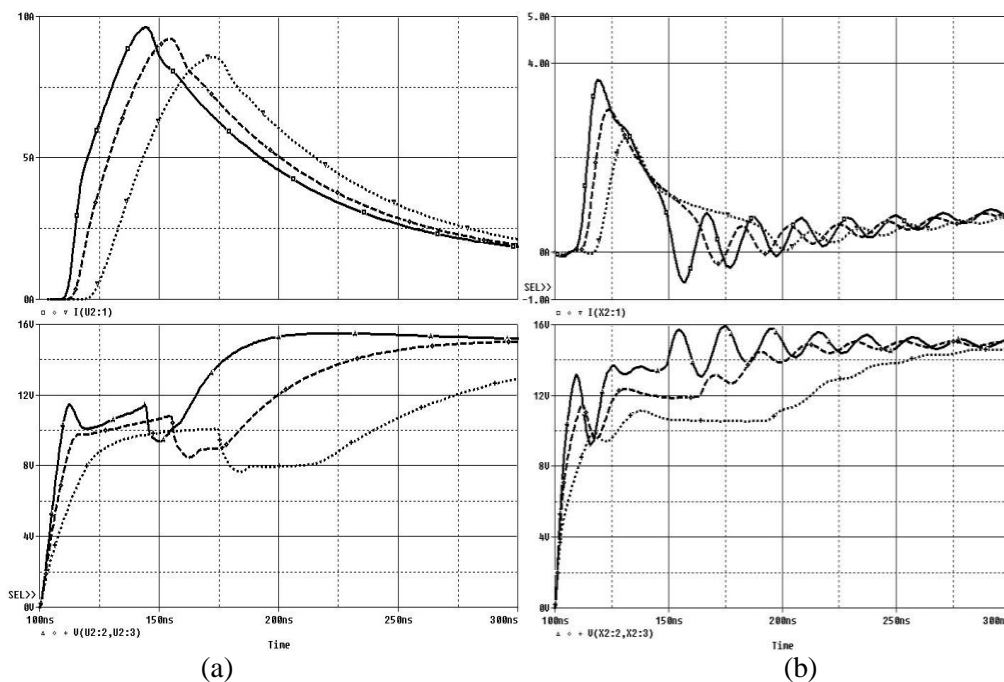(a)   (b)

Figure 19. Turn-on comparison.

Fig. 20 compares IGBT (a) and MOSFET (b) turn-off dynamics at various gate resistance.

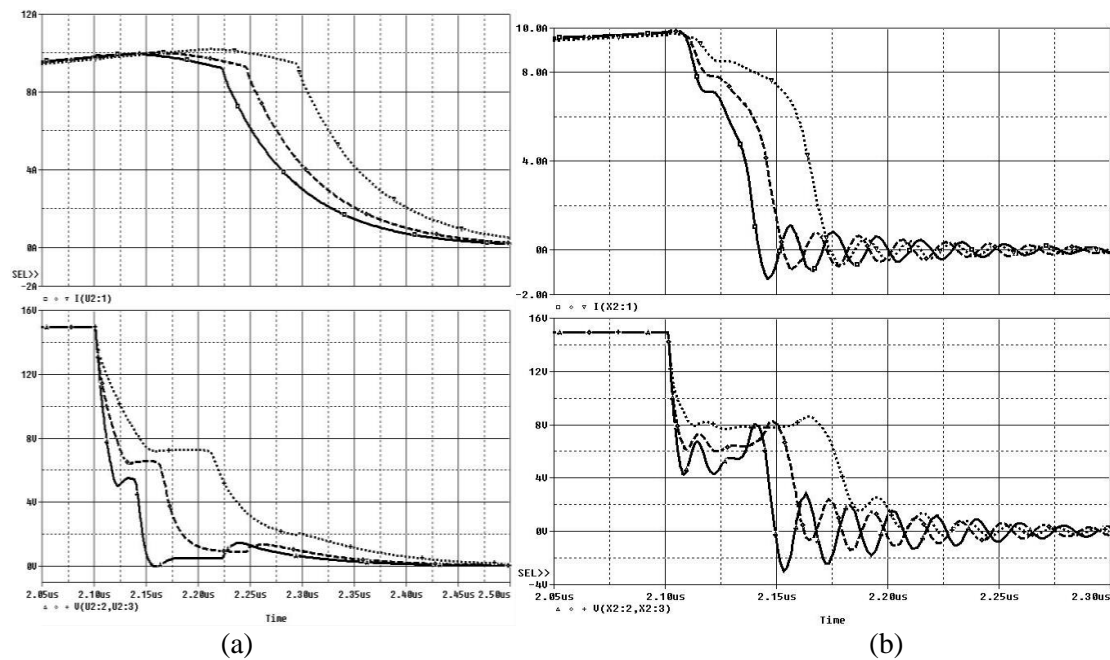(a)   (b)

Figure 20. Turn-off comparison.

On the top the current is shown, on the bottom the V_{GE}/V_{GS}. Solid lines are referred to RG = 5 Ω, dashed lines are referred to RG = 10 Ω and dotted lines are referred to RG = 20 Ω. As in turn-on dynamics, the higher the gate resistance, the smoother the characteristics but turn-off time increases. At last the energy losses as a function of gate resistance are shown in Fig. 21.

Figure 21. Switching Losses.

4 c) Reverse recovery diodes characterization

Fig. 22 shows the forward characteristics (I_F vs V_F) of reverse recovery diode at various junction temperatures. For this simulation it has been necessary to add a third IGBT and MOSFET in the test circuit. Solid lines with square symbols show Si-diode characteristics and dashed lines with "x" symbols show SiC-diode characteristics.

Figure 22. Forward characteristics of intrinsic diode.

The dynamic behaviour is shown in Fig. 23 for each device, top graph for Si-diode and bottom graph for SiC diode.

Figure 23. Reverse recovery behaviour of intrinsic diode.

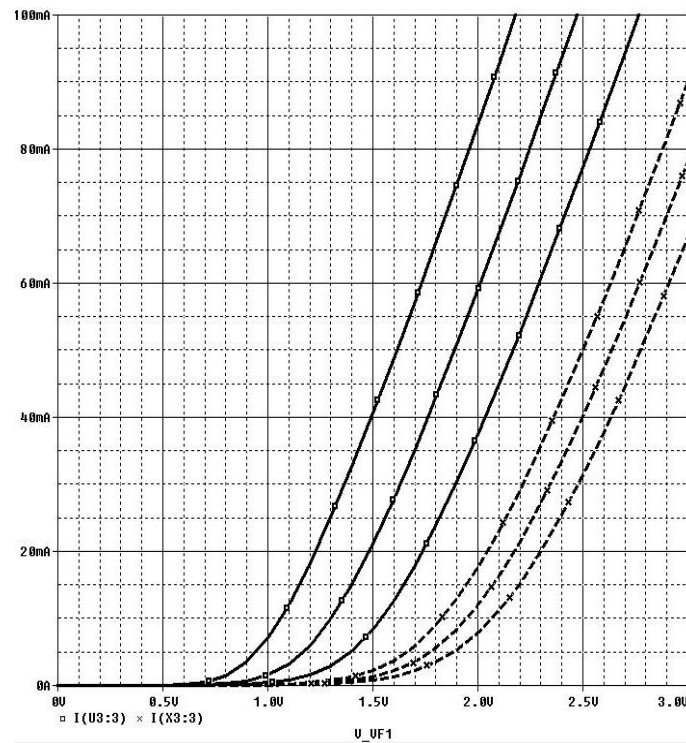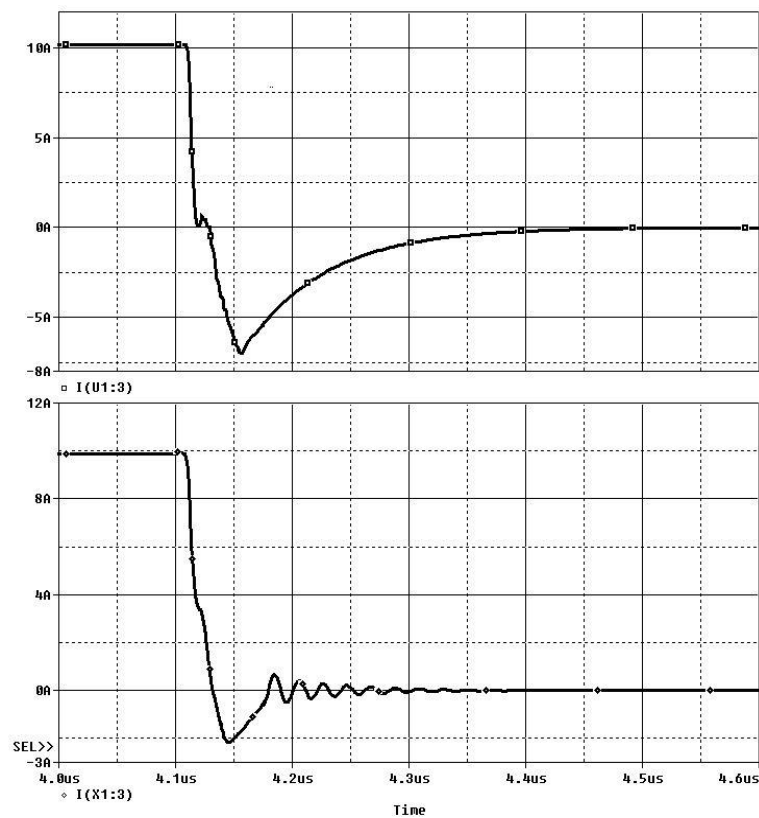## V.   CONCLUSIONS

The state of art of the main types of semiconductors devices for Industrial PWM Inverters has been presented. In particular we have examined the last generations of Silicon Carbide (SiC) MOSFETs and Insulated Gate Bipolar Transistors (IGBTs). SPICE simulations for static characteristics have been evaluated at different temperatures while dynamic ones have been performed at different gate resistance, in order to identify the device which makes the PWM inverter more efficient.

Contrary to Si-IGBTs, no tail current was noticed for SiC-MOSFET leading to high switching capabilities for these devices. The SiC MOSFET showed superior performance in terms of switching as well as conduction loss but ringing effect may cause some problems.

REFERENCES

[1]   T. Fujihira, et al., "The State-of-The-Art and Future Trend of Power Semiconductor Devices," Proceedings of PCIM Europe 2015, pp. 27-34, Nuremberg, Germany, 19 - 21 May 2015.

[2]   K. V. Kumar, et al., "Simulation and comparison of SPWM and SVPWM control for three phase inverter," ARPN Journal of Engineering and Applied Sciences, vol. 5, no. 7, pp. 62-74, 2010.

[3]   J. Caldwell, "Analog Pulse Width Modulation (SLAU508)," Texas Instruments, 2013.

[4]   M. L. H. I. B. B. N. M. N. M. A. S. A. H. Zulkifilie Bin Ibrahim, "Simulation Investigation of SPWM, THIPWM and SVPWM Techniques for Three Phase Voltage Source Inverter," International Journal of Power Electronics and Drive System (IJPEDS), vol. 4, no. 2, pp. 223-232, 2014.

[5]   J. Holtz, "Pulse Width Modulation for Electronic Power Conversion," Proceedings of the IEEE, vol. 82, no. 8, pp. 1194-1214, 1994.

[6]   B. Cao and L. Chang, "A Variable Switching Frequency Algorithm to Improve the Total Efficiency of Single-Phase Grid-Connected Inverters," Applied Power Electronics Conference and Exposition (APEC), 2013 Twenty-Eighth Annual IEEE, pp. 2310-1315, 2013.

[7]   A. G. Perri, "Fondamenti di Dispositivi Elettronici," Ed. Progedit, Bari, Italy, ISBN 978-88-6194-080-2, 2016.

[8]   A. G. Perri, "Dispositivi Elettronici Avanzati," Ed. Progedit, Bari, Italy, ISBN 978-88-6194-081-9, 2016.

[9]   R. Vaid and N. Padha, "Comparative Study of Power MOSFET device structures," Indian Journal of Pure & Applied Physics, vol. 43, pp. 980-988, 2005.

[10]   "Power MOSFET Basics," ALPHA & OMEGA Semiconductor, http://www.aosmd.com/products, 2016.

[11]   A. Sattar, "IXYS Power MOSFET Products (IXAN0062)," IXYS Corporation, http://ixdev.ixys.com.

[12]   A. Elasser and T. P. Chow, "Silicon Carbide Benefits and Advantages for Power Electronics Circuits and Systems," Proceedings of the IEEE, vol. 90, no. 6, pp. 969-986, 2002.

[13]   J. B. Casady, et al., "New Generation 10 kV SiC Power MOSFET and Diodes for Industrial Applications," Proceedings of PCIM Europe 2015, Nuremberg, Germany, 19 - 21 May 2015.

[14]   A. Sattar, "Insulated Gate Bipolar Transistor (IGBT) Basics (IXAN0063)," IXYS Corporation, http://ixdev.ixys.com.

[15]   "IGBT Fundamentals," SIEMENS Semiconductor Group.

[16]   E. R. Motto, , et al., "Characteristics of a 1200V PT IGBT With Trench Gate and Local Life Time Control," 1998 Industry Applications Conference, vol. 2, pp. 811-816, 1998.

[17]   T. Heinzel, et al., "The New High Power Density 7th Generation IGBT Module for Compact Power Conversion Systems," Proceedings of PCIM Europe 2015, pp. 1-9, Nuremberg, Germany, 19 - 21 May 2015.

[18]   "STGW15H120DF2 Datasheet (DocID023751 Rev 5)," ST Microelectronics, 2015.

[19]   "SCT20N120 Datasheet (DocID026413 Rev 4)," ST Microelectronics, 2015.

[20]   K. Peng, et al., "Characterization and Modeling of SiC MOSFET Body Diode," 2016 IEEE Applied Power Electronics Conference and Exposition (APEC), pp. 2127-2135, 2016.

[21]   M. Nawaz and K. Ilves, "On the comparative assessment of 1.7 kV, 300 A full SiC-MOSFET and Si-IGBT power modules," 2016 IEEE Applied Power Electronics Conference and Exposition (APEC), pp. 276-282, 2016.

AUTHORS

Gianluca Sena received the B. S. degree in information engineering, curriculum electronics, from Università del Salento, Lecce (Italy), in 2011.
He worked from 2012 to 2015 in Power Electronics R&D Group of Energy Factory Bari, an integrated multidisciplinary laboratory for research activities in aerospace and energy fields.
Actually he is a student of M. S. course of electronics engineering of Polytechnic University of Bari (Italy) and he works in the Electronic Device Laboratory of Bari Polytechnic for the design and realization of energy conversion systems.

Roberto Marani received the Master of Science degree *cum laude* in Electronic Engineering from Polytechnic University of Bari, where he received his Ph.D. degree in Electronic Engineering. He worked in the Electronic Device Laboratory of Bari Polytechnic for the design, realization and testing of nanoelectronic systems. Moreover he worked in the field of design, modelling and experimental characterization of devices and systems for biomedical applications.
Currently Dr. Marani is a Reseacher of the National Research Council of Italy (CNR), at the Institute of Intelligent Systems for Automation (Bari).
He has published over 160 book chapters, journal articles and conference papers and serves as referee for many international journals.

Anna Gina Perri received the Laurea degree *cum laude* in Electrical Engineering from the University of Bari in 1977. In the same year she joined the Electrical and Electronic Department, Polytechnic University of Bari, Italy, where she is Full Professor of Electronics from 2002.
In 2004 she was awarded the "Attestato di Merito" by ASSIPE (ASSociazione Italiana per la Progettazione Elettronica), Milano, BIAS'04, for her studies on electronic systems for domiciliary teleassistance.
Her current research activities are in the area of numerical modelling and performance simulation techniques of electronic devices for the design of GaAs Integrated Circuits and in the characterization and design of optoelectronic devices on PBG (Phothonic BandGap). Moreover she works in the design, realization and testing of nanometrical electronic systems, quantum devices, FET on carbon nanotube and in the field of experimental characterization of electronic systems for biomedical applications.
Prof. Perri is the Head of the Electron Devices Laboratory of the Polytechnic University of Bari.
She is author of over 250 journal articles, conference presentations, twelve books and currently serves as a Referee of a number of international journals.
Prof. Perri is the holder of two italian patents and the Editor of three international books.
She is also responsible for research projects, sponsored by the Italian Government.
Prof. Perri is an Associate Member of National University Consortium for Telecommunications (CNIT).